

# QUO VADIS: QoS-aware Underwater Optimization Framework for Inter-vehicle Communication using Acoustic Directional Transducers

Baozhi Chen and Dario Pompili

Department of Electrical and Computer Engineering, Rutgers University, New Brunswick, NJ

Emails: baozhi\_chen@cac.rutgers.edu, pompili@ece.rutgers.edu

**Abstract**—Underwater acoustic communications consume a significant amount of energy due to the high transmission power (10 – 50 W) and long data packet transmission times (0.1 – 1 s). Mobile Autonomous Underwater Vehicles (AUVs) can conserve energy by waiting for the ‘best’ network topology configuration, e.g., a *favorable alignment*, before starting to communicate. Due to the frequency-selective underwater acoustic ambient noise and high medium power absorption – which increases exponentially with distance – a shorter distance between AUVs translates into a lower transmission loss and a higher available bandwidth. By leveraging the predictability of AUV trajectories, a novel solution is proposed that optimizes communications by delaying packet transmissions in order to wait for a favorable network topology (thus trading end-to-end delay for energy and/or throughput). In addition, the solution proposed – which is implemented and compared with other solutions using an emulator that integrates underwater acoustic WHOI Micro-Modems – exploits the frequency-dependent radiation pattern of underwater acoustic transducers to reduce communication energy consumption by adjusting the transducer directivity on-the-fly.

## I. INTRODUCTION

UnderWater Acoustic Sensor Networks (UW-ASNs) [1] have been deployed to carry out collaborative monitoring tasks including oceanographic data collection, disaster prevention, and navigation. To enable advanced underwater explorations, Autonomous Underwater Vehicles (AUVs), equipped with underwater sensors, are used for information gathering. Underwater *gliders* are one type of battery-powered AUVs that use hydraulic pumps to vary their volume in order to generate the buoyancy changes that power their forward gliding. These gliders are designed to rely on local intelligence with minimal onshore operator dependence. Due to propagation limitations of Radio Frequency (RF) and optical waves, i.e., high medium absorption and scattering respectively, acoustic communication technology is employed to transfer vital information (data and configuration) between gliders underwater and, ultimately, to a surface station where this information is gathered and analyzed.

Position information is of vital importance in mobile underwater sensor networks, as the data collected has to be associated with appropriate location in order to be spatially reconstructed onshore. Even though AUVs can surface periodically (e.g., every few hours) to locate themselves using Global Positioning System (GPS) – *which does not work underwater* – over time, inaccuracies in models for deriving position estimates, self-localization errors, and drifting due to ocean currents will

significantly increase the uncertainty in position of underwater vehicle. Such uncertainty may degrade the quality of collected data and also the efficiency, reliability, and data rates of underwater inter-vehicle communications [2], [3].

Besides the need to associate sensor data with 3D positions, in fact, position information can also be helpful for underwater communications. For example, underwater geographic routing protocols (e.g., [4]–[6]) assume the positions of the nodes are known. AUVs involved in exploratory missions usually follow predictable trajectories, e.g., gliders follow *sawtooth* trajectories, which can be used to predict position and, therefore, to improve communication. By leveraging the predictability of the AUVs’

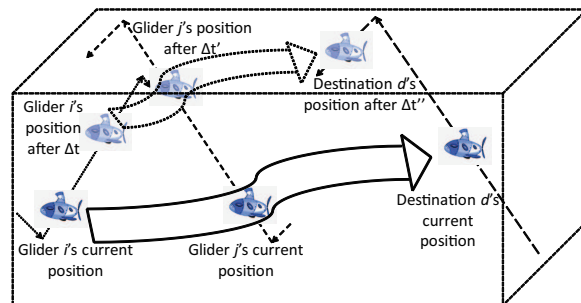


Fig. 1. Glider  $i$  delays its transmission by  $\Delta t$  waiting for a better topology so to improve energy and/or throughput to destination  $d$ . Wide arrows represent the packet forwarding routes and dashed/dotted simple arrows represent glider trajectories.

trajectory, the energy consumption for communication can be minimized by delaying packet transmissions in order to wait for a favorable network topology, thus trading end-to-end (e2e) delay for energy and/or throughput<sup>1</sup>. For instance, Fig. 1 depicts a scenario where glider  $i$  waits for a certain time period  $\Delta t$  [s] to save transmission energy and to achieve higher throughput. Based on  $j$ 's and  $d$ 's trajectory, glider  $i$  predicts a ‘better’ topology with relatively shorter links after  $\Delta t$  and postpones transmission in favor of lower transmission energy and higher data rate. This approach differs from that proposed for Delay Tolerant Networks (DTNs), where delaying transmission becomes necessary to overcome the temporary lack of network connectivity [8], [9].

<sup>1</sup>Due to the peculiar ‘V’ shape of the underwater acoustic ambient noise and the high medium power absorption exponentially increasing with distance [7], a shorter distance between AUVs translates into a lower transmission loss and a higher available bandwidth.

To estimate an AUV's position, in [10] we proposed a statistical approach to estimate a glider's trajectory. The estimates were used to minimize e2e energy consumption for networks where packets in the queue need to be forwarded right away (delay-sensitive traffic). In this work, we focus on delay-tolerant traffic and propose an optimization framework that uses acoustic directional transducers to reduce the computation and communication overhead for inter-vehicle data transmission. Moreover, we offer the distinction between two forms of position uncertainty depending on the network point of view, i.e., *internal* and *external uncertainty*, which refer to the position uncertainty associated with a particular entity/node (such as an AUV) as seen *by itself* or *by others*, respectively (see Sect. IV-A for more details). By distinguishing between internal and external uncertainty, the causes of the position uncertainty can be understood and different components of the position uncertainty can be modeled and derived. Solutions can further be designed to reduce the uncertainty of different components so that such uncertainty can be minimized for network performance improvement.

Based on the estimated external uncertainty, in this paper we propose QUO VADIS<sup>2</sup>, a **Q**oS-aware **u**nderwater **o**ptimization framework for inter-vehicle communication using **a**coustic **d**irectional transducers. QUO VADIS is a cross-layer optimization framework for delay-tolerant UW-ASNs that jointly considers the e2e delay requirements and constraints of underwater acoustic communication modems, including transducer directivity, power control, packet length, modulation, and coding schemes. Specifically, the proposed framework uses the external-uncertainty region estimates of the gliders and forwards delay-tolerant traffic where the maximum e2e delay is large: *Class I (delay-tolerant, loss-tolerant)* and *Class II (delay-tolerant, loss-sensitive)* [6]. Moreover, our cross-layer communication framework exploits the frequency-dependent radiation pattern of underwater acoustic transducers. By decreasing the frequency band, transducers can change their "directivity" turning from being almost omnidirectional (with a gain of  $\approx 0$  dBi) – which is a desirable feature to support neighbor discovery and multicasting, geocasting, anycasting, and broadcasting) – to directional (with gains up to 10 dBi) – which is useful for long-haul unicast transmissions.

The contribution of this paper is as follows:

- We offer the distinction between two forms of position uncertainty (internal and external, depending on the view of the different nodes). A static approach is then proposed to estimate the position uncertainty and this estimated uncertainty is then used to improve network performance.
- We exploit the frequency dependent directivity of the acoustic transducer that is originally used as omnidirectional transducer at one frequency to optimize network performance.
- We propose a distributed communication framework for delay-tolerant applications where AUVs can conserve energy by waiting for a 'good' network topology configuration, e.g., a *favorable alignment*, before starting to communicate.

The remainder of this paper is organized as follows. In

Sect. II, we review the related work for delay-tolerant networks, for communication solutions using directional transducers, and for cross-layer optimization frameworks in UW-ASNs. We present the underwater communication model in Sect. III and propose our solution, QUO VADIS, in Sect. IV. In Sect. V, performance evaluation and analysis are carried out, while conclusions are discussed in Sect. VI.

## II. RELATED WORK

Solutions for DTNs have been proposed for communications within extreme and performance-challenged environments where continuous e2e connectivity does not hold most of the time [8], [9]. Many approaches as summarized by [11] are mainly focused on solutions for intermittently connected terrestrial networks. Several solutions for UW-ASNs have been proposed in [12]–[15].

In [12], an energy-efficient protocol is proposed for such delay-tolerant data-retrieval applications. Efficient erasure codes and Low Density Parity Check (LDPC) codes are also used to reduce Packet Error Rate (PER) in the underwater environment. In [13], an adaptive routing algorithm exploiting message redundancy and resource reallocation is proposed so that 'more important' packets can obtain more resources than other packets. Simulation results showed that this approach can provide differentiated packet delivery according to application requirements and can achieve a good e2e performance trade-off among delivery ratio, average e2e delay, and energy consumption. A Prediction Assisted Single-copy Routing (PASR) scheme that can be instantiated for different mobility models is proposed in [14]. An effective greedy algorithm is adopted to capture the features of network mobility patterns and to provide guidance on how to use historical information. It is shown that the proposed scheme is energy efficient and cognizant of the underlying mobility patterns.

In [15], an approach called Delay-tolerant Data Dolphin (DDD) is proposed to exploit the mobility of a small number of capable collector nodes (namely dolphins) to harvest information sensed by low power sensor devices while saving sensor battery power. DDD performs only one-hop transmissions to avoid energy-costly multi-hop relaying. Simulation results showed that limited numbers of dolphins can achieve good data-collection requirements in most application scenarios. However, data collection may take a long time as the nodes need to wait until a dolphin moves into the communication ranges of these nodes.

Compared to the number of approaches using directional antennae for terrestrial wireless sensor networks, solutions using directional transducers for UW-ASNs are very limited due to the complexity of estimating position and direction of vehicles underwater. Moreover, these solutions generally assume the transducers are ideally directional. That is, they assume the radiation energy of the transducer is focused on some angle range with no leaking of radiation energy outside this range. For example, such transducers are used for localization using directional beacons in [16] and for directional packet forwarding in [17]. These solutions also use only one frequency. In this work, rather than using the ideal transducer model, we consider the radiation patterns of existing real-world

<sup>2</sup>"Quo vadis?" is a Latin phrase meaning "Where are you going?".

transducers at different frequencies in order to minimize energy consumption.

A cross-layer optimization solution for UW-ASNs has been proposed in [6], where the interaction between routing functions and underwater characteristics is exploited, resulting in improvement in e2e network performance in terms of energy and throughput. A study on the interaction between physical and Medium Access Control (MAC) layers is presented in [18], where a method is proposed to estimate the battery lifetime and power cost for shallow-water UW-ASNs. In this way, the energy consumption is equalized and the network lifetime is prolonged. A cross-layer approach that improves energy consumption performance by jointly considering routing, MAC, and physical layer functionalities is proposed in [5]. These solutions, however, do not consider uncertainty in the AUV positions and are implemented and tested only by software simulation platforms. On the contrary, we propose a practical uncertainty-aware cross-layer solution that incorporates the functionalities of the WHOI Micro-Modem [19] to minimize energy consumption. Moreover, our solution is implemented on real hardware and tested in our emulator integrating WHOI underwater acoustic modems.

### III. NETWORK MODEL

In this section we introduce the UW-ASN that our solution is based on and state the related assumptions. Suppose the network is composed of a number of gliders, which are deployed in the ocean for long periods of time (weeks to months) to collect oceanographic data. For propulsion, they change their buoyancy using a pump and use lift on wings to convert vertical velocity into forward motion as they rise and fall through the ocean. They travel at a fairly constant horizontal speed, typically 0.25 m/s [1]. Gliders control their heading toward predefined waypoints using a magnetic compass.

Assume the gliders need to forward the data they sensed to a collecting glider. The slow-varying and mission-dependent (and, for such reasons, ‘predictable’) trajectory of a glider is used in our solution to estimate another glider’s position using the position and velocity estimate from some time earlier. A glider estimates its own trajectory and position uncertainty using its own position estimates; the parameters of the estimated trajectory and internal-uncertainty region are sent to neighboring gliders. Using these parameters, gliders can extrapolate the glider’s current position, and a confidence region accounting for possible deviation from the extrapolated course.

The Urick model is used to estimate the transmission loss  $TL(l, f)$  [dB] as,

$$TL(l, f) = \kappa \cdot 10 \log(l) + \alpha(f) \cdot l, \quad (1)$$

where  $l$  [m] is the distance between the transmitter and receiver and  $f$  [Hz] is the carrier frequency. Spreading factor  $\kappa$  is taken to be 1.5 for practical spreading, and  $\alpha(f)$  [dB/m] represents an absorption coefficient that increases with  $f$  [7].

The Urick model is a coarse approximation for underwater acoustic wave transmission loss. In reality, sound propagation speed varies with water temperature, salinity, and pressure, which causes wave paths to bend. Acoustic waves are also reflected from the surface and bottom. Such uneven propagation of waves results in *convergence (or shadow) zones*, which

are characterized by lower (or higher) transmission loss than that predicted by the Urick model due to the uneven energy dispersion. Due to space limitation, we cannot give a detailed description, but more details can be found in [20].

Due to these phenomena, the Urick model is not sufficient to describe the underwater channel for simulation purposes. The Bellhop model is based on ray/beam tracing, which can model these phenomena more accurately. This model can estimate the transmission loss by two-dimensional acoustic ray tracing for a given sound-speed depth profile or field, in ocean waveguides with flat or variable absorbing boundaries. Transmission loss is calculated by solving differential ray equations, and a numerical solution is provided by HLS Research [21]. Because the Bellhop model requires more information about the environment than a glider will have, it is only used to simulate the acoustic environment for testing (relying on trace files with historic data). Hence, the proposed solution uses the Urick model in the cross-layer optimization (Sect. IV-B), which can be computed online on the glider.

We adopt the empirical ambient noise model presented in [7], where a ‘V’ structure of the power spectrum density (psd) is shown. The ambient noise power is obtained by integrating the empirical psd over the frequency band in use<sup>3</sup>.

### IV. PROPOSED APPROACH

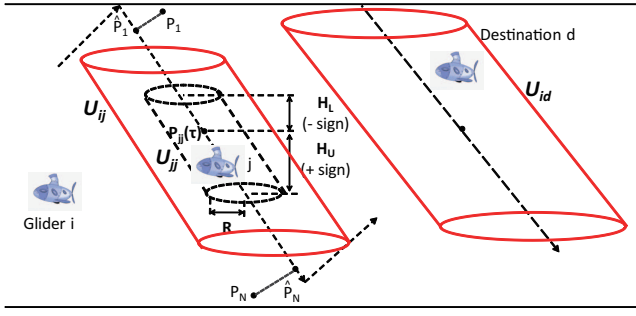
Our proposed optimization is based on the estimation of the gliders’ trajectories and their external-uncertainty regions. Therefore, in this section, we introduce the estimation of external-uncertainty regions for gliders first. We then present the cross-layer design of our proposed framework.

#### A. Internal and External Uncertainty

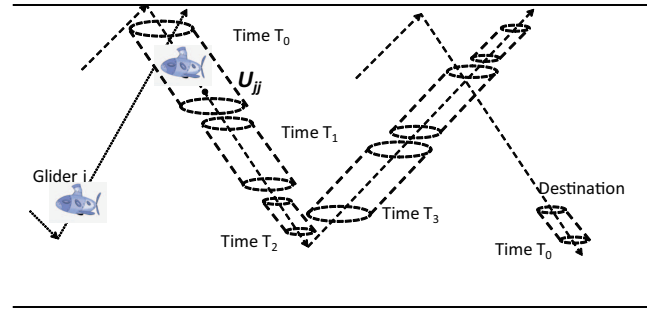
We first offer the distinction between two types of position uncertainty, followed by the discussion on the relationship between these two types of uncertainty. Finally, we present the statistical approach for external-uncertainty region estimation when gliders are used as AUVs and ocean currents are unknown.

*Internal uncertainty* refers to the position uncertainty associated with a particular entity/node (such as an AUV) *as seen by itself*. Many approaches such as those using Kalman Filter (KF) [22], [23] have been used to estimate this uncertainty assuming that the variables to be estimated have linear relationships between each other and that noise is additive and Gaussian. When the linearity assumption does not hold, there is no guarantee of optimality and non-linear filters such as the extended or unscented KF are used. These approaches attempt to minimize the mean squared errors in estimates by jointly considering the navigation location and the sensed states/features such as underwater terrain features. However, major challenges exist in extracting features from raw sensor data and in establishing the mapping between sensor data and related features (i.e., the problem of data association), which are non trivial, especially in an unstructured underwater environment.

<sup>3</sup>Note that in underwater acoustics, power (or source level) is usually expressed using decibel (dB) scale, relative to the reference pressure level in underwater acoustics  $1\mu Pa$ , i.e., the power induced by  $1\mu Pa$  pressure. The conversion expression for the source level  $SL$  re  $\mu Pa$  at the distance of 1 m of a compact source of  $P$  watts is  $SL = 170.77 + 10 \log P$  [20].



(a) Estimated internal-uncertainty region by  $j$ : a cylinder with circular bottom radius  $R$  and height  $H_U - H_L$



(b) Change of internal-uncertainty region over time.

Fig. 2. External- and internal-uncertainty regions for gliders under the effect of unknown ocean currents.

**External uncertainty**, as introduced in this paper, refers to the position uncertainty associated with a particular entity/node as seen by others. Let  $\mathcal{N}$  be the set of nodes in the network. Let us denote the internal uncertainty, a 3D region associated with any node  $j \in \mathcal{N}$ , as  $\mathcal{U}_{jj}$ , and the external uncertainties, 3D regions associated with  $j$  as seen by  $i, k \in \mathcal{N}$ , as  $\mathcal{U}_{ij}$  and  $\mathcal{U}_{kj}$ , respectively, where  $i \neq j \neq k$ . In general,  $\mathcal{U}_{jj}$ ,  $\mathcal{U}_{ij}$ , and  $\mathcal{U}_{kj}$  are different from each other; also, because symmetry does not hold,  $\mathcal{U}_{ij}$  is in general different from  $\mathcal{U}_{ji}$ . External uncertainties may be derived from the broadcast/propagated internal-uncertainty estimates (e.g., using *one-hop* or *multi-hop neighbor discovery mechanisms*) and, hence, will be affected by *e2e network latency* and *information loss*. Network latency underwater is high and is attributed to i) acoustic propagation delays, ii) transmission delays caused by a limited bandwidth that can be as low as few tens of kHz [7], and iii) delays introduced by MAC and multi-hop routing protocols, which can be up to seconds [6]. Information loss can be substantial and is attributed to packet losses caused by channel unreliability due to multipath, fading, ambient noise, and *shadow zones*.

The estimation of the external-uncertainty region  $\mathcal{U}_{ij}$  of a generic node  $j$  at another node  $i$  (with  $i \neq j$ ) involves the participation of both  $i$  and  $j$ . Node  $j$  will first estimate its positions at different points in time, its trajectory, and its internal-uncertainty region  $\mathcal{U}_{jj}$ ; then, it will broadcast the parameters describing this region in its neighborhood. Upon receiving  $j$ 's internal-uncertainty region parameters, glider  $i$  will estimate the external-uncertainty region of  $j$ ,  $\mathcal{U}_{ij}$ . Here we use the received  $\mathcal{U}_{jj}$  as  $\mathcal{U}_{ij}$  (a delayed version due to propagation delay, transmission delay and packet loss). Better estimation of  $\mathcal{U}_{ij}$  involves estimation of the change of  $\mathcal{U}_{jj}$  with time and is left as future work. We provide a solution for internal- and external-uncertainty estimation when 1) *gliders are used* (which move in a predictable 'sawtooth' trajectory) and 2) *ocean currents are unknown*.

**Internal-uncertainty estimation at  $j$ :** Assume gliders estimate their own locations over time using *dead reckoning*. Glider  $j$ 's estimated coordinates,  $P_n = (x_n, y_n, z_n)$  at sampling times  $t_n$  ( $n = 1 \dots N$ ), are used to estimate its trajectory line segment as the Orthogonal Least Square (OLS) line, which gives the best maximum likelihood estimation [24]. This trajectory segment can be described as  $P(t) = \bar{P} + \vec{v}(t - \bar{t})$ , where  $\bar{P} = (\bar{x}, \bar{y}, \bar{z}) = \frac{1}{N} \sum_{n=1}^N (x_n, y_n, z_n)$  and  $\vec{v} = \frac{\|\bar{P}_1 \bar{P}_N\|}{\|(a^*, b^*, c^*)\| \cdot (t_N - t_1)} \cdot (a^*, b^*, c^*)$ . Here,  $[a^*, b^*, c^*]^T$  is the

singular vector of matrix

$$\mathbf{A} = \begin{bmatrix} x_1 - \bar{x} & y_1 - \bar{y} & z_1 - \bar{z} \\ x_2 - \bar{x} & y_2 - \bar{y} & z_2 - \bar{z} \\ \vdots & \vdots & \vdots \\ x_N - \bar{x} & y_N - \bar{y} & z_N - \bar{z} \end{bmatrix}$$

corresponding to its largest absolute singular value,  $\bar{t} = \frac{1}{N} \sum_{n=1}^N t_n$  is the average of the sampling times, and  $\bar{P}_i$  is the projection of point  $P_i$  on the line segment (Fig. 2(a)).

After trajectory estimation, because gliders have no knowledge about the currents affecting themselves (and the other gliders), the internal-uncertainty region of  $j$  is estimated as a *cylindrical region*<sup>4</sup>. This cylinder  $\mathcal{U}$  is described by its radius  $R$  and its height  $H_U - H_L$ , where  $H_U$  and  $H_L$  – in general different – are the *signed distances* of the cylinder's top and bottom surface (i.e., the surface ahead and behind in the trajectory direction, respectively) to glider  $j$ 's expected location on the trajectory.

Using *statistical inference*, in [10] we demonstrate that:

1)  $H_L$  and  $H_U$  can be estimated as

$$\begin{cases} H_L = \bar{H} - \hat{t}_{\alpha, N-1} S^{(H)} \sqrt{1 + 1/N} \\ H_U = \bar{H} + \hat{t}_{\alpha, N-1} S^{(H)} \sqrt{1 + 1/N} \end{cases}, \quad (2)$$

where  $\bar{H} = \sum_{n=1}^N H_n / N$  is the mean of these  $N$  samples,  $S^{(H)} = [\frac{1}{N-1} \sum_{n=1}^N (H_n - \bar{H})^2]^{1/2}$  is the unbiased standard deviation,  $1 - \alpha$  is the confidence level, and  $\hat{t}_{\alpha, N-1}$  is the  $100(1 - \alpha/2)\%$  of *Student's  $t$ -distribution* [24] with  $N - 1$  degrees of freedom; and

2)  $R$  is estimated by

$$R = \frac{\sqrt{N-1} S^{(R)}}{\sqrt{\hat{\chi}_{\alpha, 2(N-1)}}}, \quad (3)$$

where  $S^{(R)} = [\frac{1}{N-1} \sum_{n=1}^N (R_n - \bar{R})^2]^{1/2}$ ,  $\bar{R} = \frac{1}{N} \sum_{n=1}^N R_n$ , and  $\hat{\chi}_{\alpha, 2(N-1)}$  is the  $100(1 - \alpha)\%$  of  $\chi$ -distribution with  $2(N - 1)$  degrees of freedom. As shown in Fig. 2(b),  $j$ 's internal-uncertainty region becomes smaller over time (from  $T_0$  to  $T_2$ ), i.e., as more position estimates are acquired.

<sup>4</sup>If the ocean current moves in any direction in the 3D space,  $j$ 's drifting can be treated as a 3D Brownian Motion where the deviations in  $x$  and  $y$  direction are identically independently distributed (i.i.d.), which makes the horizontal projection of  $j$ 's confidence region circular. And as  $j$  moves along its ascending or descending trajectory, the region swept is a cylinder. Although the pressure sensor on  $j$  gives a rather accurate vertical position, there still can be vertical uncertainty due to 'upwelling' or 'downwelling' currents. The uncertainty-region shape can be made more realistic if some ocean-current knowledge is available.

**External-uncertainty estimation at  $i$ :** After receiving  $j$ 's trajectory and internal-uncertainty region parameters  $(\bar{P}, \bar{l}, \bar{\mathbf{v}}, H_U, H_L, R)$ , glider  $i$  can update the estimate of  $j$ 's external-uncertainty region. Note that, because AUVs involved in missions show predictable trajectories, information about the sawtooth segment can be used to derive the entire glider trajectory through extrapolation assuming symmetry between glider ascent and descent. Due to packet delays and losses in the network,  $j$ 's external-uncertainty regions as seen by single- and multi-hop neighbors are *delayed versions* of  $j$ 's own internal uncertainty (Fig. 2(b)). Hence, when using *multi-hop neighbor discovery schemes*, the internal uncertainty of a generic node  $j$ ,  $\mathcal{U}_{j,j}$ , provides a *lower bound* for all the external uncertainties associated with that node,  $\mathcal{U}_{i,j}$ ,  $\forall i \in \mathcal{N}$ . When there is an unexpected significant change in  $j$ 's trajectory,  $j$  will inform its neighbors immediately so that the other gliders will not continue to estimate the external-uncertainty region along the 'old' trajectory, i.e., before the change. If the dive and climb angles are the same, then the region estimated for the previous segment can be reused for estimating the new segment. In our solution, a higher queueing priority is assigned to broadcast packets containing this change of course information.

### B. Cross-layer Optimization for Delay-tolerant Applications

With the external-uncertainty regions, a glider needs to select an appropriate neighbor to forward each packet to its final destination. Because the major part of available energy in battery-powered gliders should be devoted to propulsion [25], acoustic communications should not take a large portion of the available energy. Our proposed protocol minimizes the energy spent to send a message to its destination and considers the functionalities of a real acoustic modem for a practical solution. Specifically, we provide support and differentiated service to delay-tolerant applications with different QoS requirements, from loss sensitive to loss tolerant. Hence, we consider the following two classes of traffic:

**Class I (delay-tolerant, loss-tolerant).** It may include multimedia streams that, being intended for storage or subsequent offline processing, do not need to be delivered within strict delay bounds. This class may also include scalar environmental data or non time-critical multimedia content such as snapshots. In this case, the loss of a packet is tolerable at the current hop, but its e2e PER should still be below a specified threshold.

**Class II (delay-tolerant, loss-sensitive).** It may include data from critical monitoring processes that require some form of offline post processing. In this case, a packet must be re-transmitted if it is not received correctly.

Our protocol employs only local information to make routing decisions, resulting in a scalable distributed solution (even though the destination information is required for routing, we can use the destination information learned from local neighbors to predict the position of the destination). The external-uncertainty regions obtained as described in Sect. IV-A are used to select the neighbor with minimum packet routing energy consumption. Here, a framework using the WHOI Micro-Modem [19] is presented. This framework can be extended and generalized in such a way as to incorporate the constraints of other underwater communication modems.

To be more specific, given the current time  $t_{now}$  [s] and a message  $m$  generated at time  $t_0$  [s], glider  $i$  jointly optimizes the time  $\Delta t$  [s] to wait for the best topology configuration, a neighbor  $j^*$ , a frequency band  $f_{ij}$ , transmission power  $P_{TX}^{(i,j)}(t)$  [W], packet type  $\xi$ , and number of frames<sup>5</sup>  $N_F$ , so that the estimated energy  $E_{id}(t)$  [J] to route  $m$  to destined glider  $d$ 's region  $\mathcal{U}_{id}$  is minimized and message  $m$  reaches it within  $B_{max}$  [s], the maximum e2e delay from the source to the destination. We assume power control is possible in the range  $[P_{min}, P_{max}]$  although transmission power is currently fixed for the WHOI Micro-Modem. We anticipate more advanced amplifier hardware will make this power optimization possible.

Here,  $E_{id}(t)$  is estimated by the energy to transmit the packet to neighbor  $j$  in one transmission, the average number of transmissions  $\hat{N}_{TX}^{(i,j)}(t)$  to send  $m$  to  $j$ , and the estimated number of hops  $\hat{N}_{hop}^{(j,d)}(t)$  to reach region  $\mathcal{U}_{id}$  via  $j$ . We need to estimate the transmission power and the number of hops to destination. The external-uncertainty region is used to estimate the number of hops  $\hat{N}_{hop}^{(j,d)}(t)$  to  $d$  via neighbor  $j$  and the lower bound of the transmission power as follows (Fig. 3). Let  $\hat{l}_{i,p_1,p_2}(t)$  [m] be the projected distance of line segment from  $i$  to position  $p_1$  on the line from  $i$  to position  $p_2$ , and  $l_{i,p}(t)$  be the distance from  $i$  to position  $p$ .  $\hat{N}_{hop}^{(j,d)}(t)$  is estimated by the worst case of  $l_{i,p}(t)/\hat{l}_{i,p_1,p_2}(t)$ , i.e., (8). The lower bound for transmission power is estimated by the average transmission power so that the received power at every point in  $\mathcal{U}_{i,j}$  is above the specified threshold  $P_{TH}$ . The transmission power lower bound is the integral of the product of the transmission power to obtain  $P_{TH}$  at a point in  $\mathcal{U}_{i,j}$  and the probability density function (pdf) of  $j$  to be at this point.

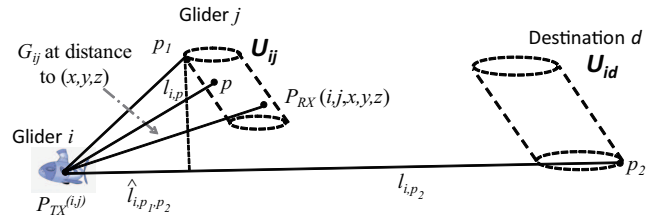


Fig. 3. Use of external-uncertainty region in the optimization framework.

To estimate the received power, it is necessary to estimate the transducer gains at the transmitter and receiver. To estimate the transmitter's gain  $G_{TX}(\theta_{ij}, \phi_{ij}, f_{ij})$ ,  $i$  needs to compute the radiation angles – the horizontal angle  $\theta_{ij} \in [-180^\circ, 180^\circ]$  and the vertical angle  $\phi_{ij} \in [-90^\circ, 90^\circ]$  with respect to  $j$ . Assume the initial position of the transducer is as shown in the top left corner of Fig. 4, then  $i$ 's normalized transducer direction vector is  $\vec{\mathbf{n}}_i = (0, 0, -1)$  with the *horizontal plane*  $z = z_0^{(i)}$  (defined as the plane perpendicular to  $\vec{\mathbf{n}}_i$ ). While the glider is moving, its pitch, yaw, and roll angles are denoted by  $\varepsilon_i$ ,  $\zeta_i$ , and  $\eta_i$ , respectively. From geometry, the direction vector after rotation is  $\vec{\mathbf{n}}_i = \mathbf{Q}_x(\eta_i)\mathbf{Q}_y(\zeta_i)\mathbf{Q}_z(\varepsilon_i)\vec{\mathbf{n}}_i^T$ , while the transducer's horizontal plane is  $\mathbf{Q}_x(-\eta_i)\mathbf{Q}_y(-\zeta_i)\mathbf{Q}_z(-\varepsilon_i)[x, y, z]^T = z_0^{(i)}$ , where  $z_0^{(i)}$  is a constant, and  $\mathbf{Q}_x(\eta_i)$ ,  $\mathbf{Q}_y(\zeta_i)$  and  $\mathbf{Q}_z(\varepsilon_i)$  are

$$\begin{bmatrix} 1 & 0 & 0 \\ 0 & \cos \eta_i & -\sin \eta_i \\ 0 & \sin \eta_i & \cos \eta_i \end{bmatrix}, \begin{bmatrix} \cos \zeta_i & 0 & -\sin \zeta_i \\ 0 & 1 & 0 \\ \sin \zeta_i & 0 & \cos \zeta_i \end{bmatrix}, \begin{bmatrix} \cos \varepsilon_i & -\sin \varepsilon_i & 0 \\ \sin \varepsilon_i & \cos \varepsilon_i & 0 \\ 0 & 0 & 1 \end{bmatrix},$$

respectively.

<sup>5</sup>Each packet sent by WHOI Micro-Modem consists of a number of frames.

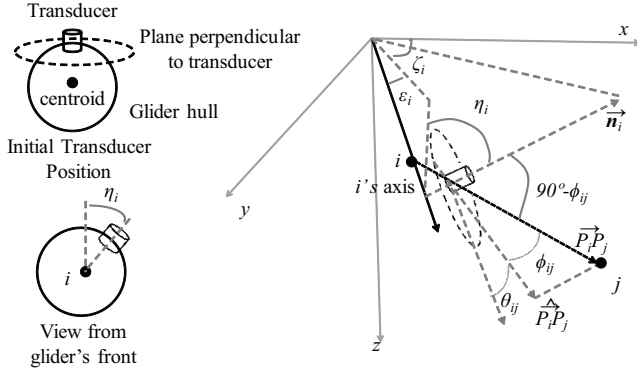


Fig. 4. Derivation of transducer angles from glider  $i$  to  $j$ .

With the position vector  $\overrightarrow{P_i P_j}$  from  $i$  to  $j$ , we can derive  $\cos \phi_{ij} = \frac{\widehat{\overrightarrow{P_i P_j}} \circ \overrightarrow{P_i P_j}}{\|\widehat{\overrightarrow{P_i P_j}}\| \cdot \|\overrightarrow{P_i P_j}\|}$  and  $\cos \theta_{ij} = \frac{\widehat{\overrightarrow{P_i P_j}} \circ \overrightarrow{\mathbf{v}}_i}{\|\widehat{\overrightarrow{P_i P_j}}\| \cdot \|\overrightarrow{\mathbf{v}}_i\|}$ , where  $\widehat{\overrightarrow{P_i P_j}}$  is the projection of  $\overrightarrow{P_i P_j}$  on the transducer's horizontal plane,  $\circ$  is the inner product, and  $\overrightarrow{\mathbf{v}}_i = \|\overrightarrow{\mathbf{v}}_i\| \cdot [\cos \varepsilon_i \cos \zeta_i, \cos \varepsilon_i \sin \zeta_i, \sin \varepsilon_i] = (a_i^*, b_i^*, c_i^*)$  is the velocity vector of glider  $i$  as estimated in Sect. IV-A. As  $\overrightarrow{\mathbf{n}}_i$  is perpendicular to the transducer's horizontal plane, we have  $\sin \phi_{ij} = \cos(90 - \phi_{ij}) = \frac{\overrightarrow{\mathbf{n}}_i \circ \overrightarrow{P_i P_j}}{\|\overrightarrow{\mathbf{n}}_i\| \cdot \|\overrightarrow{P_i P_j}\|}$  and  $\widehat{\overrightarrow{P_i P_j}} = \overrightarrow{P_i P_j} - (\overrightarrow{P_i P_j} \circ \overrightarrow{\mathbf{n}}_i) \cdot \overrightarrow{\mathbf{n}}_i$ . The transducer's gain at receiver  $j$ ,  $G_{RX}(\theta_{ji}, \phi_{ji}, f_{ij})$ , can be estimated in a similar way.

Let  $L_m(\xi)$  be  $m$ 's length in bits depending on packet type  $\xi$  and  $B(\xi)$  be the corresponding bit rate. The energy to transmit the packet to neighbor  $j$  in one transmission can therefore be approximated by  $P_{TX}^{(i,j)}(t) \cdot \frac{L_m(\xi)}{B(\xi)}$ .

Overall, the optimization problem can be formulated as **P(i, d, t<sub>now</sub>, Δt<sub>p</sub>): Cross-layer Optimization Problem**

**Given:**  $P_{min}, P_{max}, \Xi, \Omega_\xi, G_{TX}(), G_{RX}(), \eta, B_{max}, PER_{max}^{e2e}$

**Computed:**  $\varepsilon_i, \zeta_i, \varepsilon_j, \zeta_j, \mathcal{U}_{ij}, \forall j \in \mathcal{N}_i \cup \{d\}$  (i.e.,  $R_j^{(i)}, H_L^{(i,j)}, H_H^{(i,j)}$ )

**Find:**  $j^* \in \mathcal{N}_i, P_{TX}^{(i,j)^*}(t) \in [P_{min}, P_{max}], \xi^* \in \Xi, N_F^* \in \Omega_\xi, \Delta t^*, f_{ij}^* \in [f_L, f_U]$

**Minimize:**  $E_{id}(t) = P_{TX}^{(i,j)}(t) \cdot \frac{L_m(\xi)}{B(\xi)} \cdot \hat{N}_{TX}^{(i,j)}(t) \cdot \hat{N}_{hop}^{(j,d)}(t)$  (4)

**Subject to:**

**(class-independent relationships)**

$$t = t_{now} + \Delta t; \quad (5)$$

$$t_{TTL} = B_{max} - (t_{now} - t_0); \quad (6)$$

$$L_m(\xi) = L_F(\xi) \cdot N_F + L_H; \quad (7)$$

$$\hat{N}_{hop}^{(j,d)}(t) = \frac{\max_{p \in \mathcal{U}_{id}} l_{i,p}(t)}{\min_{p_1 \in \mathcal{U}_{ij}, p_2 \in \mathcal{U}_{id}} \hat{l}_{i,p_1,p_2}(t)}; \quad (8)$$

$$SINR_{ij}(t) = \frac{P_{TX}^{(i,j)}(t) \cdot 10^{G_{ij}(l_{ij}(t), f_{ij})/10}}{\sum_{k \in \mathcal{A} \setminus \{i\}} P_{TX}^{(k,j)}(t) \cdot 10^{G_{ij}(l_{kj}(t), f_{ij})/10} + N_0}; \quad (9)$$

$$G_{ij}(l_{ij}, f_{ij}) = G_{TX}(\theta_{ij}, \phi_{ij}, f_{ij}) + G_{RX}(\theta_{ji}, \phi_{ji}, f_{ij}) - L_{AMP}(f_{ij}) - TL(l_{ij}, f_{ij}); \quad (10)$$

$$\theta_{ij} = \arcsin \frac{\overrightarrow{\mathbf{n}}_i \circ \overrightarrow{P_i P_j}}{\|\overrightarrow{P_i P_j}\|}; \quad (11)$$

$$\phi_{ij} = \arccos \frac{\widehat{\overrightarrow{P_i P_j}} \circ \overrightarrow{\mathbf{v}}_i}{\|\widehat{\overrightarrow{P_i P_j}}\| \cdot \|\overrightarrow{\mathbf{v}}_i\|}. \quad (12)$$

In this formulation,  $\mathcal{N}_i$ ,  $\Xi$ , and  $\Omega_\xi$  denote the set of  $i$ 's neighbors, the set of packet types, and the set of number of type  $\xi$  frames respectively;  $L_F(\xi)$  [bit] is the length of a frame of type  $\xi$ ,  $L_H$  [bit] is the length of message  $m$ 's header;  $PER(SINR_{ij}(t), \xi)$  is the PER of type  $\xi$  at the Signal to Interference-plus-Noise Ratio  $SINR_{ij}(t)$ ,  $TL(l_{ij}(t), f_{ij})$  is the transmission loss for distance  $l_{ij}(t)$  and carrier frequency  $f_{ij}$  [kHz] – which is calculated using (1) –  $\mathcal{A} \setminus \{i\}$  is the set of active transmitters excluding  $i$ , and  $P_{TX}^{(i,j)}(t)$  is the transmission power used by  $i$  to reach  $j$ .

Note that  $N_0 = \int_{f_L}^{f_U} psd_{N_0}(f, w) df$  is the ambient noise, where  $psd_{N_0}(f, w)$  is the empirical noise power spectral density (psd) for frequency band  $[f_L, f_U]$  and  $w$  [m/s] is the surface wind speed as in [7].  $t_{TTL}$  is the remaining Time-To-Live (TTL) for the packet,  $L_{AMP}(f_{ij})$  [dB] is the power loss of the power amplifier at  $f_{ij}$  and  $PER_{max}^{e2e}$  is the maximum e2e error rate for packet  $m$ .

The objective function (4) estimates the energy required to send message  $m$  to the destination region  $\mathcal{U}_{id}$ ; (5) is the time after waiting  $\Delta t$ ; (6) calculates the remaining TTL for message  $m$ ; (7) calculates the total message's length; (8) estimates the number of hops  $\hat{N}_{hop}^{(i,j)}(t)$  to reach destination  $d$ ; (9) estimates the SINR at  $j$  while (10) estimates the total transmission gain in dB from  $i$  to  $j$ , including the transducer gain at the transmitter and receiver, loss at the power amplifier, and transmission loss; (11) and (12) estimate the transducer's radiation angles of  $j$  with respect to  $i$ . The constraints for **P(i, d, t<sub>now</sub>, Δt<sub>p</sub>)** are,

**(class-independent constraints)**

$$P_{TX}^{(i,j)}(t) \geq \int_{(x,y,z) \in \mathcal{U}_{id}} P_{RX}(i, j, x, y, z) \cdot 10^{-G_{ij}(l_{ij}(t), f_{ij})/10} \cdot pdf_R(x, y) \cdot pdf_H(z) dx dy dz; \quad (13)$$

$$P_{RX}(i, j, x, y, z) \geq P_{TH}; \quad (14)$$

$$0 \leq \Delta t \leq \frac{t_{TTL}}{\hat{N}_{TX}^{(i,j)}(t) \cdot \hat{N}_{hop}^{(j,d)}(t)}. \quad (15)$$

In these constraints,  $P_{RX}(i, j, x, y, z)$  is the received signal power at the generic 3D location  $(x, y, z)$  when  $i$  transmits to  $j$ . Last,  $pdf_R(x, y)$  and  $pdf_H(z)$  are the pdfs of the glider's position on the horizontal plane (i.e.,  $\chi$ -distribution with degree of  $2N - 2$ ) and on the vertical direction (i.e., Student's  $t$ -distribution with  $N - 1$  degrees of freedom), respectively [10],  $P_{TH}$  is the received power threshold so that the packet can be received with a certain predefined probability. (13) estimates the lower bound of the transmission power to cover the external-uncertainty region so that the received power is above a pre-specified threshold, as accounted for in (14); (15) estimates the bounds of  $\Delta t$ , which must be less than the maximum tolerable delay at the current hop. To support the two classes of delay-tolerant traffic, we have the following additional constraints,

**(additional class-dependent constraints)**

$$\text{Class I} = \begin{cases} \hat{N}_{TX}^{(i,j)}(t) = 1 \\ 1 - [1 - PER(SINR_{ij}(t), \xi)]^{\hat{N}_{hop}^{(j,d)}(t)} \leq PER_{max}^{e2e} \end{cases}$$

$$\text{Class II} = \left\{ \hat{N}_{TX}^{(i,j)}(t) = [1 - PER(SINR_{ij}(t), \xi)]^{-1} \right.$$

The first constraint for Class I traffic forces packet  $m$  to be transmitted only once, while the second constraint guarantees the e2e PER of  $m$  should be less than a specified threshold  $PER_{max}^{e2e}$ . The constraint for Class II traffic guarantees message  $m$  will be transmitted for the average number of times for successful reception at  $j$ . By solving this local optimization

problem every time the inputs change significantly (and not every time a packet needs to be sent),  $i$  is able to select the optimal next hop  $j^*$  so that message  $m$  is routed (using minimum network energy) to the external-uncertainty region  $\mathcal{U}_{i,d}$  where destination  $d$  should be. Obviously different objective functions (e2e delay, delivery ratio, throughput) could be used depending on the traffic class and mission QoS requirements. Note that in fact our solution can be extended to serve two other classes of traffic - 1) delay-sensitive, loss-tolerant traffic, and 2) delay-sensitive, loss-sensitive traffic - by setting  $B_{\max}$  to the minimum e2e delay.

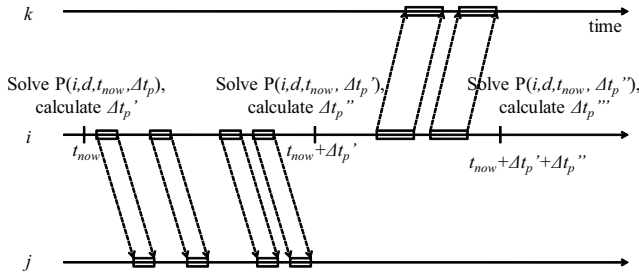


Fig. 5. Solving  $\mathbf{P}(i, d, t_{\text{now}}, \Delta t_p)$  every  $\Delta t_p$  at  $i$ .

To reduce the complexity, we can convert  $\mathbf{P}(i, d, t_{\text{now}}, \Delta t_p)$  into a discrete optimization problem by considering finite sets of  $P_{TX}^{(i,j)}$  and  $\Delta t$ , which can be taken to be a number of equally spaced values within their respective ranges. The problem then can be solved by comparing the e2e energy consumption estimates of different combination of these discrete values. The embedded Gumstix motherboard (400 MHz processor and 64 MB RAM) attached to the Micro-Modem is adequate to solve such a problem. To further reduce the computation, instead of running the solution for every packet, it will be rerun only at  $t_{\text{now}} + \Delta t_p$  for the same class of traffic flow that is sent from  $i$  to the same destination  $d$ . Here,  $\Delta t_p$  is taken as the minimum of the  $\Delta t$  values of the packets belonging to the same class of traffic and the same destination, estimated from the previous run. Figure 5 depicts an example of how  $\mathbf{P}(i, d, t_{\text{now}}, \Delta t_p)$  is solved at  $i$ . At time  $t_{\text{now}}$ , the problem is solved with  $j$  found to be the next hop to  $d$ . The minimum of the  $\Delta t$  values of these packets belonging to the same class of traffic and the same destination observed before  $t_{\text{now}}$  is  $\Delta t_p'$ . Packets for  $d$  will then be forwarded to  $j$  with the calculated transmission power at the selected frequency band until  $t_{\text{now}} + \Delta t_p'$ . Then, the problem is solved again and  $k$  is found to be the next hop. The minimum  $\Delta t$  observed so far is  $\Delta t_p''$  and, hence, the problem will be solved at  $t_{\text{now}} + \Delta t_p' + \Delta t_p''$ .

Once the optimal frequency band is selected,  $i$  needs to notify  $j$  to switch to the selected band. A simple protocol can be used as follows. All AUVs use the same frequency band as the Common Control Channel (CCC) to tell the receiver which band is selected. A short packet or preamble with the selected band number is first sent by the transmitter using the CCC, followed by the data packet using selected frequency band after the time for the transmitter and receiver to finish frequency band switching. The receiver will first listen on the CCC, switch to the selected band embedded in the short control packet or preamble, receive the data packet, and then send back

a short ACK packet to acknowledge the reception. Finally, both sides switch back to the CCC if the transmission succeeds or the transmission times out. More sophisticated frequency-band switching protocols, which are out of the scope of this paper, can be designed to improve network performance. We rely on the Medium Access Control (MAC) scheme with the WHOI modem to send the data. Since the speed of acoustic wave underwater is very slow when compared with radio waves, the propagation delay has to be considered in order to avoid packet collisions. However, it is difficult to estimate the propagation delay since the positions are uncertain. It may not improve the performance much as the actual propagation delay may be different from the estimation. Moreover, the inter-vehicle traffic underwater is generally low. So the problem of packet collisions is not severe and hence we can just use the MAC scheme provided by the WHOI modem.

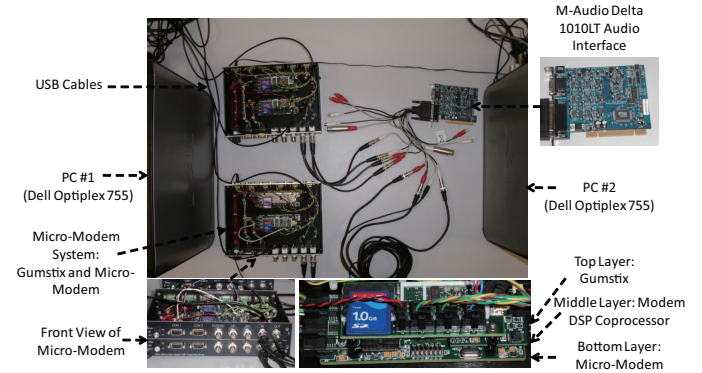


Fig. 6. Underwater communication emulator using WHOI Micro-Modems.

## V. PERFORMANCE EVALUATION

The communication solution is implemented and tested on our underwater communication emulator [10] as shown in Fig. 6. This underwater acoustic network emulator is composed of four WHOI Micro-Modems [19] and a real-time audio processing card to emulate underwater channel propagation. The multi-input multi-output audio interface can process real-time signals to adjust the acoustic signal gains, to introduce propagation delay, to mix the interfering signals, and to add ambient/man-made noise and interference. Due to the limited number of Micro-Modems and audio processing channels, we can only mix signals from up to three transmitters at the receiver modem. Therefore, we calculate, select for transmission, and mix with ambient noise, only the three most powerful signals the receiver will encounter. We leave the simulation of more than three simultaneously transmitted signals as a problem for further research.

We are interested in evaluating the performance of the proposed solution in terms of e2e energy consumption, e2e reliability (i.e., e2e delivery ratio), and average bit rate of a link, under an environment that is described by the Bellhop model (and the Munk acoustic speed profile as input).

Assume that a glider's drifting (i.e., the relative displacement from the glider's trajectory) is a 3D random process  $\{X(t), t \geq 0\}$  as the following [26]. 1) In the beginning of the deployment, the drifting is 0, i.e.,  $X(0) = (0, 0, 0)$ ; 2) The drifting has independent increments, in that for all  $0 \leq t_1 < t_2 < \dots < t_n$ ,

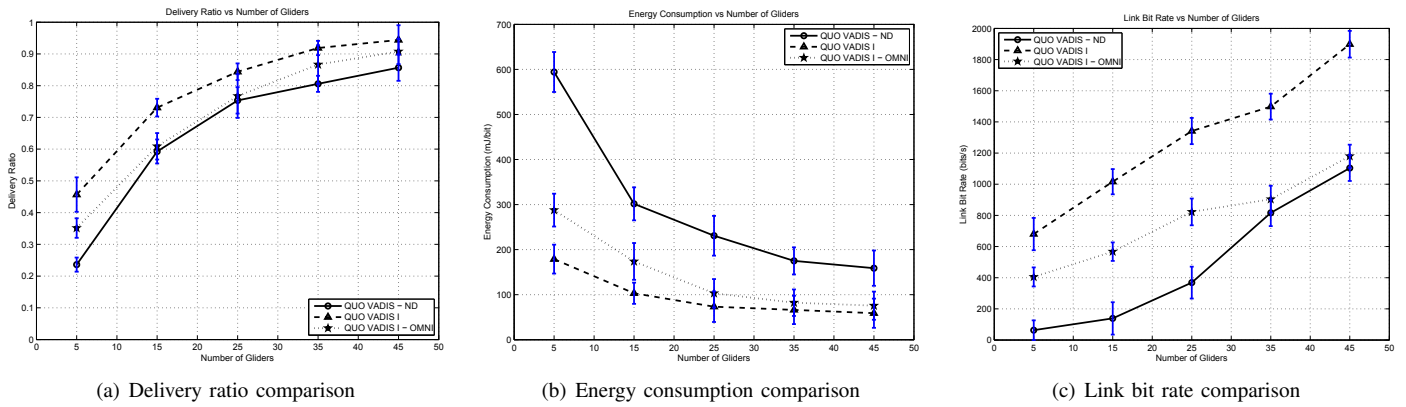


Fig. 7. Performance comparison for Class I traffic.

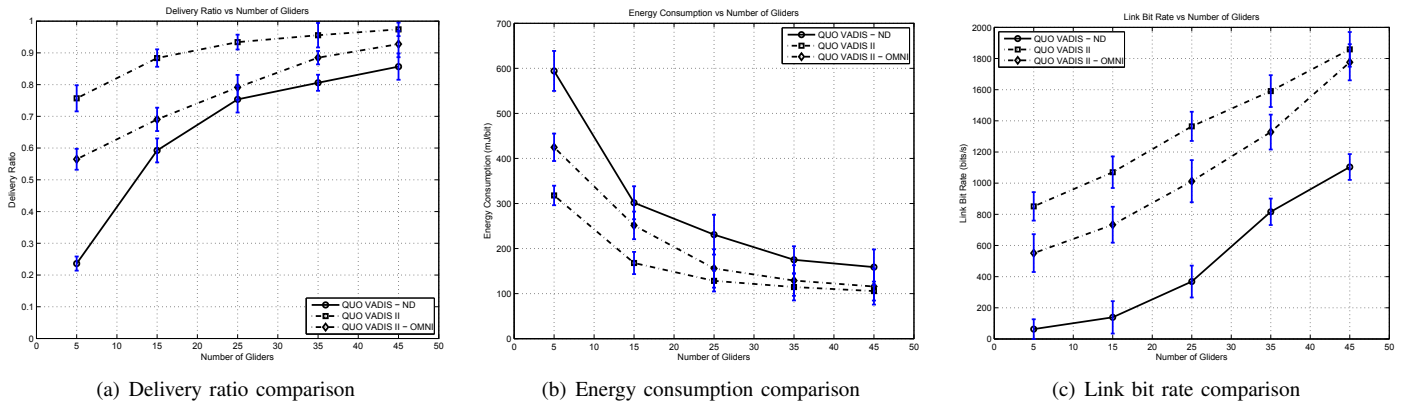


Fig. 8. Performance comparison for Class II traffic.

$X(t_n) - X(t_{n-1})$ ,  $X(t_{n-1}) - X(t_{n-1}), \dots, X(t_2) - X(t_1)$ ,  $X(t_1)$  are independent; 3) The drifting has stationary increments, in that the distribution of  $X(t+s) - X(t)$  does not depend on  $t$  and is normally distributed with zero mean and covariance matrix  $s\sigma^2 I_3$ , where  $I_3$  is the  $3 \times 3$  identity matrix, and  $\sigma$  is a scaling factor that decides the magnitude of drifting. Note that this drifting model is ideal since the drifting in any of the  $x, y, z$  directions is Gaussian. The consideration of realistic drifting pattern is left as future work. Emulation parameters are listed in Table I. The radiation pattern of the BT-25UF transducer [27] is used in the emulations. Every 10 seconds, a packet is generated in each node. A glider is randomly selected as the collector and half of the other gliders are randomly selected to forward their packets towards it. For statistical relevance, emulations are run for 50 rounds and the average is plotted with 95% confidence interval.

We are interested in evaluating the performance of our solution for the two classes of traffic in Sect. IV-B, using either the BT-25UF transducer or an ideal omni-directional transducer (with gain equal to 0 dBi). We also want to compare the performance of our solution, which delays the transmission for optimal topology configuration, with the solution without delaying the transmission. For convenience, we denote QUO VADIS for Class I traffic using the BT-25UF transducer, for Class I traffic using the ideal omni-directional transducer, for Class II traffic using the BT-25UF transducer, for Class I traffic using the ideal omni-directional transducer, the solu-

TABLE I  
EMULATION PARAMETERS

Parameter	Value
Deployment 3D region	2500(L) $\times$ 2500(W) $\times$ 1000(H) m <sup>3</sup>
Confidence Parameter $\alpha$	0.05
$[P_{min}, P_{max}]$	[1, 10] W
Packet Types $\Xi$	{0, 2, 3, 5}
Glider Horizontal Speed	0.3 m/s
Gliding Depth Range	[0, 100] m
Carrier Frequencies	10, 15, 25 kHz
$B_{max}$	10 hr

tion with no delaying of the transmission (i.e.,  $\Delta t = 0$  for  $P(i, d, t_{now}, \Delta t_p)$ ) by ‘QUO VADIS I’, ‘QUO VADIS I - OMNI’, ‘QUO VADIS II’, ‘QUO VADIS II - OMNI’, and ‘QUO VADIS - ND’.

The following networking metrics are compared:

- **e2e energy consumption:** the average energy consumed to route one bit of data to the destination;
- **e2e delivery ratio:** the number of data packets received correctly over the number of data packets sent;
- **link bit rate:** the average bit rate between a transmission pair.

Emulation results for these metrics are plotted in Figs. 7 and 8. The following is observed:

- By delaying packet transmissions to wait for the optimal network topology, the e2e energy consumption is reduced

while the e2e delivery ratio and link bit rate increase (e.g., with 5 gliders, the energy consumption for QUO VADIS I is around 30% of that for QUO VADIS-ND).

- Our proposed solution using the BT-25UF transducer has better performance, in terms of e2e energy consumption, e2e delivery ratio, and link bit rate, than that using the omni-directional transducer.
- Class II traffic has higher e2e delivery ratio than Class I traffic due to the retransmissions. On the other hand, this leads to more energy consumption.

To sum up, our proposed framework QUO VADIS improves the network performance for delay-tolerant applications in terms of e2e energy consumption, delivery ratio, and link bit rate by waiting for a ‘favorable’ topology configuration and by exploiting the gains of directional transducers.

## VI. CONCLUSION

We proposed QUO VADIS, a QoS-aware underwater optimization framework for inter-vehicle communication using acoustic directional transducers. Based on the trajectory and position uncertainties of the AUVs, an AUV predicts a favorable network topology with relatively short links in the future and postpones transmission in favor of a lower transmission energy and a higher data rate. Communication energy consumption is further reduced by exploiting the frequency-dependent radiation pattern of underwater acoustic transducers. The proposed solution is implemented and tested in our underwater communication emulator, showing improvement over protocols with no delay or protocols using omni-directional transducers in terms of e2e energy consumption, reliability, and link bit rate.

## REFERENCES

- [1] I. F. Akyildiz, D. Pompili, and T. Melodia, “Underwater Acoustic Sensor Networks: Research Challenges,” *Ad Hoc Networks (Elsevier)*, vol. 3, no. 3, pp. 257–279, May 2005.
- [2] D. Son, A. Helmy, and B. Krishnamachari, “The Effect of Mobility-induced Location Errors on Geographic Routing in Mobile Ad Hoc and Sensor Networks: Analysis and Improvement using Mobility Prediction,” *IEEE Trans. on Mobile Computing*, vol. 3, no. 3, pp. 233–245, Jul. 2004.
- [3] X. Xiang, Z. Zhou, and X. Wang, “Self-Adaptive On Demand Geographic Routing Protocols for Mobile Ad Hoc Networks,” in *Proc. of IEEE International Conference on Computer Communications (INFOCOM)*, Anchorage, AL, May 2007.
- [4] E. A. Carlson, P.-P. Beaujean, and E. An, “Location-Aware Routing Protocol for Underwater Acoustic Networks,” in *Proc. of IEEE International Conference on Engineering in the Ocean Environment (OCEANS)*, Boston, MA, Sep. 2006.
- [5] J. M. Montana, M. Stojanovic, and M. Zorzi, “Focused Beam Routing Protocol for Underwater Acoustic Networks,” in *Proc. of ACM International Workshop on Underwater Networks (WUWNet)*, San Francisco, CA, Sep. 2008.
- [6] D. Pompili and I. F. Akyildiz, “A Cross-layer Communication Solution for Multimedia Applications in Underwater Acoustic Sensor Networks,” in *Proc. of IEEE International Conference on Mobile Ad-hoc and Sensor systems (MASS)*, Atlanta, GA, Oct. 2008.
- [7] M. Stojanovic, “On the Relationship Between Capacity and Distance in an Underwater Acoustic Communication Channel,” in *Proc. of ACM International Workshop on UnderWater Networks (WUWNet)*, Los Angeles, CA, Sep. 2006.
- [8] K. Fall, “A Delay-Tolerant Network Architecture for Challenged Internets,” in *Proc. of ACM Special Interest Group on Data Communication (SIGCOMM)*, Karlsruhe, Germany, Aug. 2003.
- [9] S. Burleigh, A. Hooke, L. Torgerson, K. Fall, V. Cerf, B. Durst, K. Scott, and H. Weiss, “Delay-Tolerant Networking: An Approach to Interplanetary Internet,” *IEEE Communications Magazine*, vol. 41, no. 6, p. 128C136, Jun. 2003.

- [10] B. Chen, P. Hickey, and D. Pompili, “Trajectory-aware Communication Solution for Underwater Gliders using WHOI Micro-Modems,” in *Proc. of IEEE Communications Society Conference on Sensor, Mesh, and Ad Hoc Communications and Networks (SECON)*, Boston, MA, Jun. 2010.
- [11] Z. Zhang, “Routing in intermittently connected mobile ad hoc networks and delay tolerant networks: overview and challenges,” *IEEE Communications Surveys and Tutorials*, vol. 8, no. 1, pp. 24–37, Jan. 2006.
- [12] C. Y. Chan and M. Motani, “An Integrated Energy Efficient Data Retrieval Protocol for Underwater Delay Tolerant Networks,” in *Proc. of IEEE International Conference on Engineering in the Ocean Environment (OCEANS) - Europe*, Aberdeen, Scotland, Jun. 2007.
- [13] Z. Guo, G. Colombi, B. Wang, J.-H. Cui, and D. Maggiorini, “Adaptive Routing in Underwater Delay/Disruption Tolerant Sensor Networks,” in *Proc. of IEEE/IFIP Conference on Wireless on Demand Network Systems and Services (WONS)*, Garmisch-Partenkirchen, Germany, Jan. 2008.
- [14] Z. Guo, B. Wang, and J.-H. Cui, “Prediction assisted single-copy routing in underwater delay tolerant networks,” Univerity of Connecticut, Storrs, CT, Tech. Rep., 2010.
- [15] E. Magistretti, J. Kong, U. Lee, M. Gerla, P. Bellavista, and A. Corradi, “A Mobile Delay-tolerant Approach to Long-term Energy-efficient Underwater Sensor Networking,” in *Proc. of IEEE Wireless Communications and Networking Conference (WCNC)*, Kowloon, Hong Kong, Mar. 2007.
- [16] H. Luo, Z. Guo, W. Dong, F. Hong, and Y. Zhao, “LDB: Localization with Directional Beacons for Sparse 3D Underwater Acoustic Sensor Networks,” *Journal of Networks*, vol. 5, no. 1, pp. 28–38, Jan. 2010.
- [17] P. Xie, J. H. Cui, and L. Lao, “VBF: Vector-Based Forwarding Protocol for Underwater Sensor Networks,” in *Proc. of IFIP Networking*, Waterloo, Ontario, Canada, May 2005.
- [18] R. Jurdak, C. V. Lopes, and P. Baldi, “Battery lifetime estimation and optimization for underwater sensor networks,” in *IEEE Sensor Network Operations*, S. Poha, T. LaPorta, and C. Griffin, Eds. Wiley-IEEE Press, 2004.
- [19] L. Freitag, M. Grund, S. Singh, J. Partan, P. Koski, and K. Ball, “The WHOI Micro-Modem: An Acoustic Communications and Navigation System for Multiple Platforms,” in *Proc. of IEEE International Conference on Engineering in the Ocean Environment (OCEANS)*, Washington DC, Sep. 2005.
- [20] W. S. Burdick, “Underwater acoustic system analysis,” in *Prentice-Hall Signal Processing Series*, A. V. Oppenheim, Ed. Prentice-Hall, 1984, ch. 2, p. 49.
- [21] M. Porter, “BELLHOP Gaussian Beam/Finite Element Beam Code,” <http://oalib.hlsresearch.com/Rays/index.html>.
- [22] M. Blain, S. Lemieux, and R. Houde, “Implementation of a ROV navigation system using acoustic/Doppler sensors and Kalman filtering,” in *Proc. of IEEE International Conference on Engineering in the Ocean Environment (OCEANS)*, San Diego, CA, Sep. 2003.
- [23] S. Williams and I. Mahon, “Simultaneous localisation and mapping on the Great Barrier Reef,” in *Proc. of IEEE International Conference on Robotics and Automation (ICRA)*, New Orleans, LA, Apr. 2004.
- [24] G. Casella and R. L. Berger, *Statistical Inference*, 2nd ed. Duxbury Press, 2001.
- [25] J. Partan, J. Kurose, and B. N. Levine, “A Survey of Practical Issues in Underwater Networks,” in *Proc. of ACM International Workshop on UnderWater Networks (WUWNet)*, Los Angeles, CA, Sep. 2006.
- [26] S. M. Ross, *Introduction to Probability Models*, 8th ed. Academic Press, 2003.
- [27] L. BTech Acoustics, “BT-25UF transducer specifications,” <http://acomms.whoi.edu/documents/211006-SPC%20BT25-UF%2025kHz%20Feed%20Through%20Transducer.pdf>.